CFH Haploinsufficiency and Complement Alterations in Early-Onset Macular Degeneration

Rayne R. Lim,[1] Sharlene Shirali,[1] Jessica Rowlan,[1] Abbi L. Engel,[2] Marcos Nazario, Jr.,[1] Kelie Gonzalez,[1] Aspen Tong,[1] Jay Neitz,[1] Maureen Neitz,[1] and Jennifer R. Chao[1,3]

[1]Department of Ophthalmology, University of Washington, Seattle, Washington, United States
[2]Center for Developmental Biology and Regenerative Medicine, Seattle Children's Institute, Seattle, Washington, United States
[3]Roger and Angie Karalis Johnson Retina Center, University of Washington School of Medicine, Seattle, Washington, United States

Correspondence: Rayne R. Lim, Department of Ophthalmology, University of Washington, 750 Republican St., Box 358058, Seattle, WA 98109, USA; raynelim@uw.edu.
Jennifer R. Chao, Department of Ophthalmology, University of Washington, 750 Republican St., Box 358058, Seattle, WA 98109, USA; jrchao@uw.edu.

Received: December 1, 2023
Accepted: April 3, 2024
Published: April 29, 2024

Citation: Lim RR, Shirali S, Rowlan J, et al. CFH haploinsufficiency and complement alterations in early-onset macular degeneration. *Invest Ophthalmol Vis Sci.* 2024;65(4):43. https://doi.org/10.1167/iovs.65.4.43

Purpose. Complement dysregulation is a key component in the pathogenesis of age-related macular degeneration (AMD) and related diseases such as early-onset macular drusen (EOMD). Although genetic variants of complement factor H (CFH) are associated with AMD risk, the impact of CFH and factor H-like protein 1 (FHL-1) expression on local complement activity in human retinal pigment epithelium (RPE) remains unclear.

Methods. We identified a novel CFH variant in a family with EOMD and generated patient induced pluripotent stem cell (iPSC)-derived RPE cells. We assessed CFH and FHL-1 cofactor activity through C3b breakdown assays and measured complement activation by immunostaining for membrane attack complex (MAC) formation. Expression of CFH, FHL-1, local alternative pathway (AP) components, and regulators of complement activation (RCA) in EOMD RPE cells was determined by quantitative PCR, western blot, and immunostaining. Isogenic EOMD (cEOMD) RPE was generated using CRISPR/Cas9 gene editing.

Results. The CFH variant (c.351-2A>G) resulted in loss of CFH and FHL-1 expression and significantly reduced CFH and FHL-1 protein expression (~50%) in EOMD iPSC RPE cells. These cells exhibited increased MAC deposition upon exposure to normal human serum. Under inflammatory or oxidative stress conditions, CFH and FHL-1 expression in EOMD RPE cells paralleled that of controls, whereas RCA expression, including MAC formation inhibitors, was elevated. CRISPR/Cas9 correction restored CFH/FHL-1 expression and mitigated alternative pathway complement activity in cEOMD RPE cells.

Conclusions. Identification of a novel CFH variant in patients with EOMD resulting in reduced CFH and FHL-1 and increased local complement activity in EOMD iPSC RPE supports the involvement of CFH haploinsufficiency in EOMD pathogenesis.

Keywords: retinal pigmented epithelium, complement factor H, factor H-like protein 1, complement, induced pluripotent stem cells, age-related macular degeneration, early-onset macular drusen

Age-related macular degeneration (AMD) is the leading cause of vision loss in people 50 years and older, and it is projected to affect up to 288 million people by 2040.[1] Although strongly associated with aging, the pathogenesis of AMD is multifactorial, and the development of an effective treatment for the non-neovascular (dry) form remains a challenge. Elevated complement activity is implicated in the pathogenesis of AMD,[2] and the *Y402H* genetic variant of complement factor H (CFH) is associated with a fivefold increased risk, making it one of the strongest susceptibility genes for AMD.[3] Genetic variants in other complement components such as C2, C3, and complement factor B are linked to intermediate to late-stage disease progression.[4]

CFH is a major regulator of the alternative pathway of the complement system.[5] Retinal pigmented epithelial (RPE) cells produce both classical and alternative pathway components, including C3, complement factor B (CFB), and factor D, although additional complement factors C6 to C9 are needed for C5b-9 membrane attack complex formation.[6] The primary mechanism through which complement facilitates the immune response is through the amplification loop via C3 activation, and it is the major site of CFH action. CFH inhibits the alternative pathway by directly binding and inactivating C3b, aiding C3b cleavage by factor I, and expediting C3 convertase decay.[5] In aged eyes, CFH is found in Bruch's membrane, choriocapillaris, and intercapillary septa. However, during late AMD and geographic atrophy, CFH is reduced in Bruch's membrane and choroidal regions but increased in soft drusen.[7–9] Other complement components including C5, C6, C8, C9, clusterin, and vitronectin are also found in drusen of AMD globes,[10,11] indicating complement activity in sites of pathology.

Factor H-like protein 1 (FHL-1) is a short 49-kD version of the full-length 155-kD CFH protein, with an identical sequence up to exon 9, followed by a unique four-amino-acid tail. FHL-1 exhibits functional overlap with CFH in Bruch's membrane, including alternative pathway (AP) regulation and heparan sulfate proteoglycan binding.[12] Despite its relatively minor contribution to systemic AP regulation,[12,13] the small size and lack of glycosylation[14] of FHL-1 enable free diffusion across Bruch's membrane.[15] Generally reduced diffusion across an aged Bruch's membrane suggests that complement regulators secreted from the RPE may play an outsized role in local AP regulation in AMD.[15] Further, evidence that CFH and FHL-1 respond differently to inflammatory mediators[16] supports investigation of both isoforms.

Early-onset macular drusen (EOMD) is a monogenic autosomal dominant disease that is phenotypically similar to AMD, albeit occasionally distinguishable by its increased severity and earlier onset.[17] Rare, highly penetrant pathogenic variants in the CFH gene associated with EOMD lead to nonsense, splice-altering, or frameshift mutations that are predicted to result in loss of CFH and/or FHL-1 expression.[17] Understanding how genetic alterations in CFH/FHL-1 expression affect complement regulation in EOMD RPE cells may lead to insights into AMD pathogenesis. In this study, we describe a novel CFH variant in EOMD-affected family members and utilize patient-specific induced pluripotent stem cell (iPSC)-derived RPE for a detailed examination of alterations in local complement activity.

Methods

Generation of EOMD Patient-Derived iPSCs

Peripheral blood mononuclear cells (PBMCs) were obtained from EOMD and control participants in a University of Washington Institutional Review Board–approved protocol. Whole blood was collected from the patients, EOMD1 and EOMD2, in Vacutainer CPT tubes (Becton Dickinson, Franklin Lakes, NJ, USA) for isolation of PBMCs, which were reprogrammed into iPSCs as described previously.[18] All iPSC lines selected for study were of normal karyotype and displayed appropriate pluripotency markers (Supplementary Fig. S1). Sanger sequencing of AMD-associated variants was performed for all subjects (Supplementary Fig. S2A, Supplementary Table S1; see also Supplementary Methods).

RPE Cell Differentiation and Culture

iPSCs were cultured in either mTeSR (STEMCELL Technologies, Vancouver, BC, Canada) or Essential 8 medium (Thermo Fisher Scientific, Waltham, WA, USA). To differentiate RPE, iPSCs were split into 35-mm Matrigel-coated dishes, and differentiation was performed as previously described.[18,19] RPE cells were identified by their characteristic cobblestone morphology and pigmentation. iPSCs and RPE cells were tested negative for mycoplasm before use. RPE cells were seeded on Matrigel-coated dishes and cultured in media consisting of MEMα, 5% fetal bovine serum (FBS), N1 supplement, non-essential amino acid (NEAA), hydrocortisone, triiodothyronine, taurine, penicillin–streptomycin, and ROCK inhibitor (ROCKi, 10 µM; Selleck Chemicals, Houston, TX, USA) for the first 7 days. They were later maintained in 1% FBS without ROCKi for the remainder of the culture. For expansion and experimentation, RPE cells were seeded at 1.5×10^5cells/cm^2. Two iPSC clones were derived from each patient (EOMD1 and EOMD2) for a total of four iPSC clones. Each iPSC clone was then differentiated on two separate occasions, for a total of eight iPSC–RPE lines (four iPSC–RPE lines each from EOMD 1 and EOMD2). For age-matched controls, one iPSC clone was generated from Control1 and differentiated into RPE on two separate occasions. Two iPSC clones were generated from Control2 and differentiated into RPE on two separate occasions. There were six total control iPSC–RPE lines. CRISPR-corrected EOMD (cEOMD) were generated from EOMD2, and one iPSC clone was differentiated into RPE on three separate occasions for a total of three cEOMD iPSC–RPE cell lines. RPE cells from 4 to 8 weeks in culture, between passages 2 to 6, were used for experiments. Specific RPE lines used for each experiment are shown in Supplementary Table S2. Control, cEOMD, and EOMD RPE cells used in comparison experiments were either of the same passage or within one passage, with most experiments conducted between passages 2 and 4.

CRISPR/Cas9 CFH Correction

iPSCs from patient EOMD2 were electroporated with Cas9, ssDNA donor, and guide RNA (GTTTTCGGGTATCAATTGCT) using Amaxa Nucleofector (Human Stem Cell Kit 2; Amaxa Biosystems, Cologne, Germany) as described elsewhere.[18] Sanger sequencing was performed to identify edited clones, and long read sequencing between CFH exons 3 and 5 were done to determine off-target effects. CRISPR–EOMD iPSCs with no off-target genetic alterations were differentiated into RPE as above.

Statistical Analysis

Data were analyzed using Prism 8 (GraphPad, Boston, MA, USA). Outlier tests were performed, and a *t*-test or Mann–Whitney test was used to compare between control and EOMD RPE cells. One-way ANOVA was used to compare treatment conditions among control, EOMD, and cEOMD RPE cells. Each experiment was performed with a minimum of three cell lines in each RPE group, and at least three technical replicates were performed. In the figure legends, "n" represents technical replicates. $P \leq 0.05$ was considered statistically significant. All data are presented as mean ± SEM.

Results

Drusen and Geographic Atrophy in Patients With EOMD

Family members spanning four generations with a history of drusen and early-onset vision loss were studied (Fig. 1A). EOMD1, a 69-year-old female, had a best-corrected visual acuity (BCVA) of counting fingers 3 in the right eye and 20/60 in the left. Dilated funduscopic examination revealed geographic atrophy, nummular areas of peripheral atrophy, RPE pigmentary changes, subretinal fibrosis, and crystalline drusen (Fig. 1B, Supplementary Fig. S2B). Optical coherence tomography (OCT) imaging showed RPE loss, outer retinal degeneration, pigment epithelial detachments, and subretinal deposits (Fig. 1B'). EOMD2, a 37-year-old male, had a BCVA of 20/20 in both eyes. Fundus exam and OCT imaging were notable for large soft drusen, especially dense

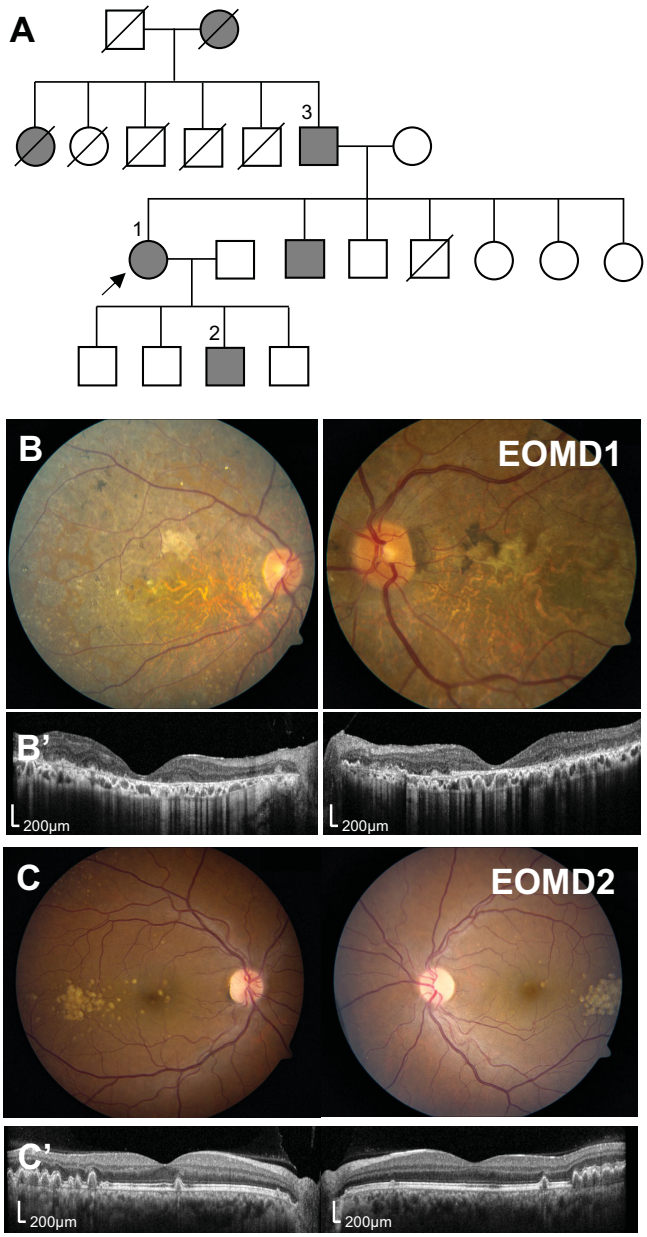

Figure 1. Patients with EOMD have distinct severity of retinal pathology. (**A**) Abridged pedigree of the EOMD family revealed familiar drusen (*filled gray boxes*) spanning four generations. Patient 1 (69 years old, female, proband), patient 2 (37 years old, male), and patient 3 (91 years old, male) were determined to have EOMD by clinical examination and Sanger sequencing. Blood was collected from EOMD1, EOMD2, and EOMD3, and iPSCs were generated from EOMD1 and EOMD2 for differentiation into RPE cells. (**B**) Fundus imaging of EOMD1 shows extensive macular geographic atrophy, nummular areas of peripheral atrophy, RPE pigmentary changes, subretinal fibrosis, and crystalline drusen. (**B'**) OCT across central macula showed RPE loss, outer retinal degeneration, and subretinal deposits. (**C**, **C'**) EOMD2 retained 20/20 visual acuity despite numerous large soft drusen in the temporal macula of both eyes.

in the temporal macula (Fig. 1C), and smaller drusen scattered throughout the peripheral retina (Supplementary Fig. S2C). Whole blood was collected from three individuals (EOMD1–3) and iPSCs were generated from EOMD1 and EOMD2.

Novel c.351-2A>G CFH Genetic Variant Results in Exon 4 Skipping and Loss of Protein Expression

Sanger sequencing of three affected individuals (EOMD1–3) revealed an A to G substitution in the 3′ splice site of exon 4 of the CFH gene (Fig. 2A). Although the canonical 3′ and 5′ splice site sequences are relatively short and poorly conserved, the AG and GT dinucleotides directly flanking the exon are absolutely conserved. FHL-1 is a splice variant and identical to CFH in exons 1 to 9, terminating in a unique four-amino-acid sequence (SFTL) encoded by exon 10. A missense mutation at the conserved 3′ splice site of exon 4 is predicted to affect both CFH and FHL-1 transcripts. Common risk alleles associated with AMD and other inherited macular drusen diseases were assessed. Although EOMD1 and EOMD 2 were homozygous for CFH *Y402H*, no other high risk alleles in *ARMS2*, *HTRA1*, *TIMP3*, *EFEMP1*, *C3*, or *CFB* were detected (Supplementary Fig. S2A).

To determine whether the c.351-2A>G variant results in the predicted splicing error, a minigene splicing assay was performed. Introns 2 to 5 from a control or corresponding genomic region from our EOMD patients were included in the FHL-1 cDNA (NM_001014975) of the minigene (Fig. 2A). After transfection of the control or EOMD minigenes into HEK293T cells, mRNA was harvested and reverse transcribed, and cDNA was amplified with primers to exons 3 and 5. The expected size of the correctly spliced minigene is 316 bp (control) (Fig. 2B). The c.351-2A>G substitution was predicted to result in exon 4 skipping, ending in a premature stop codon in exon 5. This expected mutant product size was 239 bp (exon 4 is 77 bp), which was confirmed in the minigene assay (Fig. 2B). The minor mutant product is an incorrectly spliced variant with a cryptic exon in intron 3 that does not induce a frameshift, resulting in a product size similar to the normal FHL-1 transcript (Fig. 2B). These results were confirmed by sequencing of the c.351-2A>G variant minigene transcripts (Fig. 2C). The CFH c.351-2A>G variant results in incorrect splicing of both CFH and FHL-1.

To examine whether the c.351-2A>G CFH variant leads to aberrant protein expression, we performed western blotting of secreted proteins in transfected HEK293T cells with an antibody directed toward the N-terminus of CFH and FHL-1. FHL-1 was detected in conditioned media from HEK293T cells transfected with the control minigene (49kD); however, no protein products were observed with the c.351-2A>G FHL-1 minigene (Fig. 2D). To directly determine whether mutant protein products could be produced from the incorrectly spliced transcripts, cDNA of the minor or major c.351-2A>G CFH products was cloned into vectors and transfected into HEK293T cells, and no secreted proteins were detected (Fig. 2E). These findings indicate that c.351-2A>G CFH results in loss of CFH and FHL-1 expression, and incorrectly spliced transcripts do not result in protein products.

EOMD Patient-Derived iPSC–RPE Cells Exhibited Baseline RPE Characteristics

iPSCs generated from EOMD1, EOMD2, and controls (Supplementary Fig. S1) were differentiated into RPE, as previously described.[18] iPSC–RPE cells exhibited typical orthogonal, cobblestone-like morphology, pigmentation (Figs. 3A–3C), and tight junction formation as seen with zonula occludens 1 (ZO-1) staining and transepithelial resistance (TER) measurements reaching 200 Ω·cm^2 by 3 weeks

Investigative Ophthalmology & Visual Science

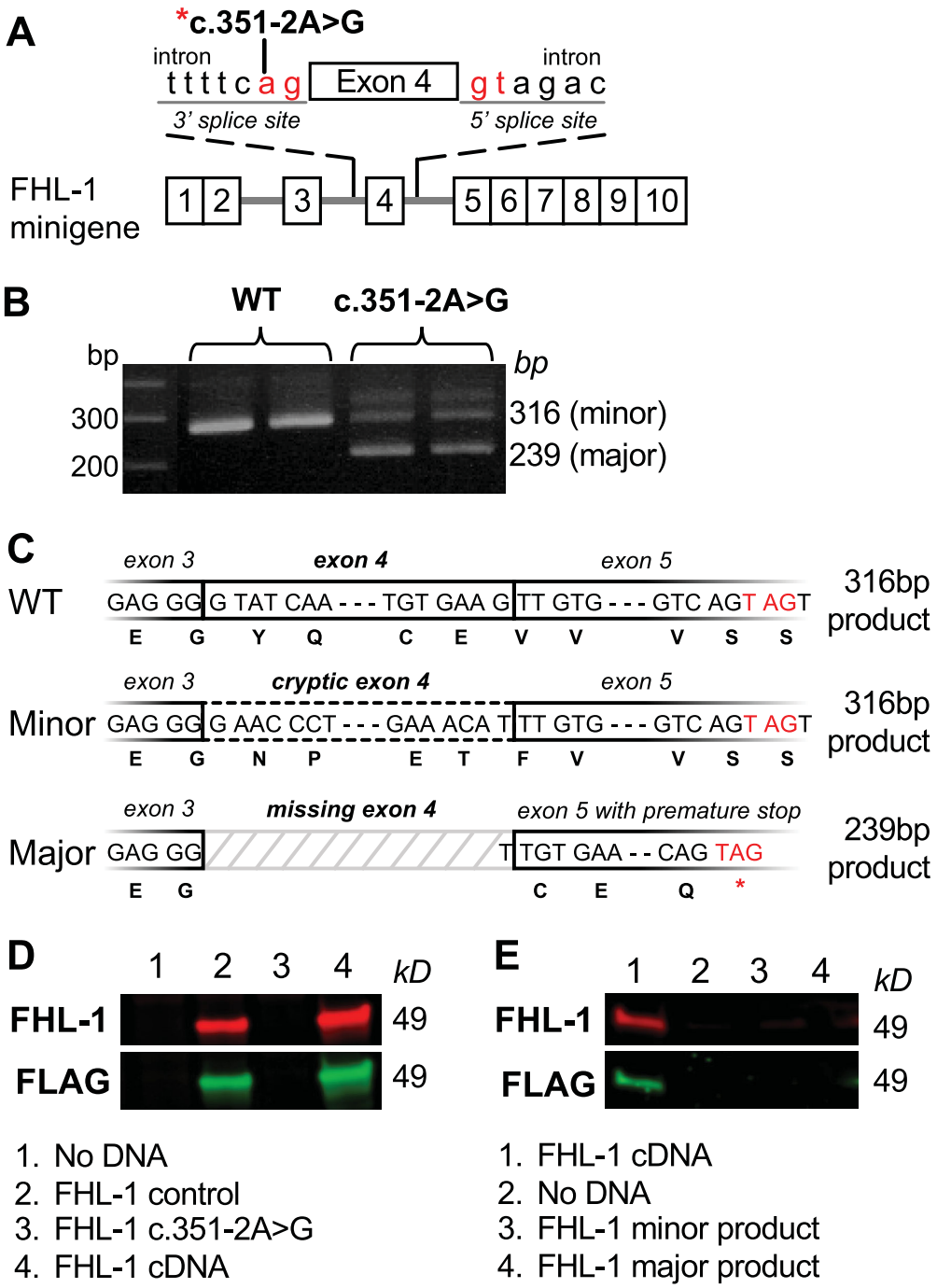

Figure 2. CFH c.351-2A>G genetic variant in EOMD patients resulted in loss of protein expression. (**A**) Sanger sequencing on patients' genomic DNA revealed an A to G substitution in conserved 3′ splice site before exon 4 of the CFH gene, which is predicted to result in splicing error affecting both CFH and FHL-1 transcripts. To validate this, HEK293T cells were transfected in a minigene splicing assay with FHL-1 cDNA plasmid containing introns between exons 2 and 5 of normal control or an EOMD patient. (**B**) After 48 hours, mRNA was isolated and reverse transcribed. PCR amplification of cDNA between exons 3 and 5 showed the expected size of the correctly spliced minigene at 316 bp. However, two transcript products at 316 bp and 239 bp were found in the c.351-2A>G–containing minigene, denoted as minor and major product according to the level of expression. (**C**) Sequencing of minor and major transcript product revealed a cryptic exon 4 from intron 3 in the minor product, whereas the major product had exon 4 skipping resulting in a premature stop codon. (**D**) Conditioned media from transfected HEK293T cells that were evaluated by western blot confirmed the absence of protein expression from the c.351-2A>G variant. (**E**) Similarly, HEK293T cells transfected with the cDNA of the minor and major transcript products did not result in detectable FHL-1 expression.

in culture (Figs. 3D–3G), as described in prior studies.[20–22] Although the expression of RPE65, MITF, LRAT2, VEGF-A, and ApoE transcripts was increased in EOMD RPE cells compared to controls (Fig. 3H), only MITF and LRAT protein expression was mildly increased (Fig. 3I). Analysis of EOMD1 and EOMD2 separately showed similar levels of protein expression (Supplementary Fig. S3A). VEGF-A secretion was polarized with higher relative basal secre-

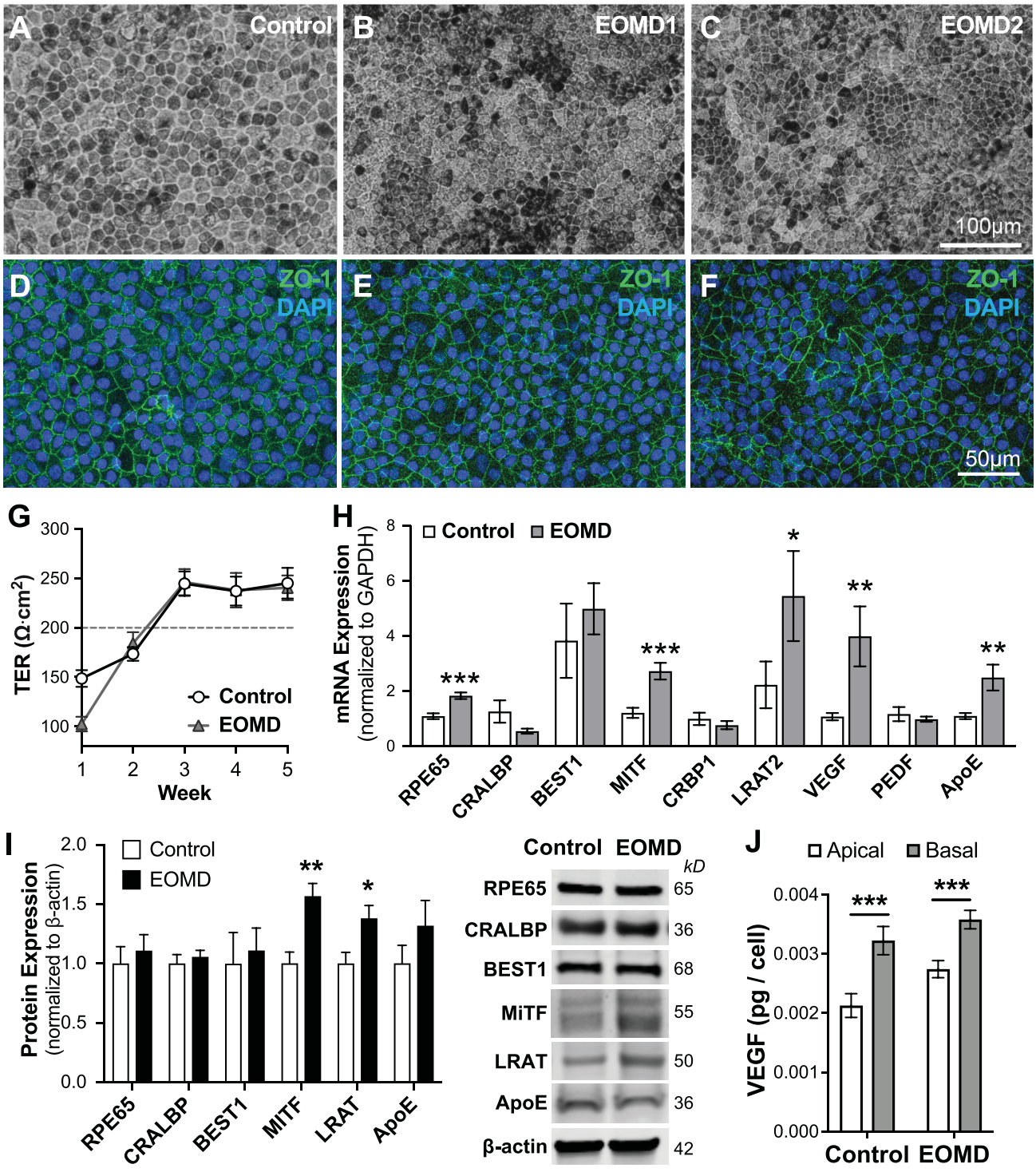

Figure 3. EOMD patient-derived iPSC–RPE cells exhibited baseline RPE characteristics. PBMC isolated from (**A**) control or (**B**, **C**) EOMD1 and EOMD2 were reprogrammed into iPSCs using episomal vectors, and subsequently differentiated into RPE cells. EOMD iPSC–RPE cells were cobblestone-like and pigmented but appeared smaller than control RPE cells despite similar seeding densities. (**D**–**F**) ZO-1 staining was consistent across all RPE cell lines. (**G**) Polarized cells on filter inserts reached TER of 200 $\Omega \cdot cm^2$ by week 3. Cells from EOMD1 and EOMD2 were cultured separately but analyzed together. (**H**) Transcript expression for RPE markers showed significant upregulation of RPE65, MITF, LRAT2, VEGF-A, and ApoE. (**I**) However, their protein expression, with the exception of MITF and LRAT, was not significantly different. (**J**) VEGF-A secretion was polarized to the basal chamber in control and EOMD RPE cells with no differences between the groups. $^{*}P < 0.05$; $^{**}P < 0.01$; $^{***}P < 0.001$ ($n = 3$).

Investigative Ophthalmology & Visual Science

tion (Fig. 3J), although there was some variability noted among inserts (Supplementary Fig. S4A). No differences were observed between the control and EOMD RPE cells after normalization to cell count.

Secreted CFH and FHL-1 Are Significantly Reduced (~50%) in EOMD iPSC–RPE Cells and Demonstrate Diminished Co-Factor Activity

CFH and FHL-1 are proteins highly secreted by the RPE, with much higher levels detected in culture media compared to cell lysate or in the extracellular matrix (ECM) (Fig. 4A, left). We found that polarized RPE cultured on filter membranes preferentially secreted CFH toward the apical chamber, and both apical and basal secretion of CFH/FHL by EOMD RPE cells was reduced (~50%) compared to controls (Figs. 4A, 4B; Supplementary Fig. S3B). Apical CFH expression was consistently higher in the polarized RPE cells on filter inserts (Supplementary Figs. S4B, S4C). The effect of decreased CFH and FHL-1 on complement activity was evaluated by measuring the breakdown of C3b. C3b is integral to common terminal pathway activation through C3 convertase formation and C5 cleavage, leading to the formation of the membrane attack complex (MAC). CFH and FHL-1 attenuate complement activity by serving as co-factors for complement factor I (CFI), which breaks down C3b.[23] In the C3b breakdown assay, CFH and FHL-1 co-factor activity is determined by the ability of exogenous CFI to cleave C3b (Fig. 4C). Successful cleavage of C3b results in iC3b products that can be visualized by electrophoresis (Fig 4D, asterisks). The iC3b breakdown products from EOMD RPE media were significantly decreased compared to controls (Figs. 4E, 4F), suggesting that baseline local complement activity in EOMD RPE cells may be elevated compared to normal controls.

EOMD RPE Cells Are More Susceptible to Oxidative Stress

RPE cells are subject to inflammatory and oxidative stressors in AMD that result in cell damage.[24] We investigated the effects of two such stressors known to have opposite effects on CFH expression in the RPE cells. Interferon-gamma (IFN-γ) is a well-characterized proinflammatory cytokine known to increase CFH in RPE cells.[25] Conversely, H_2O_2 treatment induces oxidative stress and results in decreased CFH expression via FOXO3 binding to the CFH promoter.[26] We found that IFN-γ treatment of EOMD RPE cells resulted in upregulated secretion of CFH and FHL-1, although FHL-1 expression was still significantly below that of treated controls (Fig. 5A). In contrast, H_2O_2 exposure decreased CFH and FHL-1 expression in both EOMD and control RPE cells (Fig. 5B). When calculated as a percent change in induction or suppression from naïve conditions, both stressors evoked proportionally similar, although not compensatory, responses in CFH and FHL-1 expression (Figs. 5C, 5D), suggesting haploinsufficiency in EOMD RPE cells.

A recent study showed that ~90% knockdown of CFH in human telomerase reverse transcriptase (hTERT)–RPE1 cells increased susceptibility to oxidative stress,[27] and we assessed whether an ~50% decreased expression of CFH and FHL-1 in EOMD patient-derived RPE cells would have a similar effect. After H_2O_2 exposure, cell viability was significantly reduced in EOMD RPE cells compared to controls, as determined by nuclei viability staining and release of lactate dehydrogenase (Figs. 5E, 5F). Intracellular reactive oxygen species (ROS) in EOMD RPE cells were also significantly elevated both at baseline and after H_2O_2 exposure compared to controls (Fig. 5G). Our findings suggest that decreased CFH/FHL expression may confer increased susceptibility to oxidative damage in EOMD RPE cells.

EOMD RPE Cells Have Increased Local Complement Activity and Inhibitory Regulators of Complement Activation

To determine the effects of lower levels of CFH and FHL-1 on local complement activity, EOMD and control RPE cells were treated with 10% normal human serum (NHS) to induce complement activation. In response to NHS exposure, increased MAC deposits/cell were observed compared to naïve or inactivated (HI) NHS in control RPE cells (Fig. 6A). In EOMD RPE cells, MAC deposits/cell were significantly higher both at baseline and after NHS exposure (Fig. 6B). The elevated MAC deposition, in addition to the lower C3b breakdown activity shown earlier, supports the idea that EOMD RPE cells have elevated baseline and induced local complement activity.

Regulators of complement activation (RCA) work together with CFH/FHL-1 to attenuate complement activity. CD46 (or membrane cofactor protein [MCP]) acts as a membrane-bound co-factor to CFI.[28] CD55 (or decay accelerating factor [DAF]) inactivates C3 and C5 convertases by dissociation and prevents their formation.[29] Vitronectin and clusterin are found in drusen and basal laminar deposits in human AMD globes[11,18] and, in addition to CD59, independently inhibit MAC formation.[30,31] Of the five RCA components examined, we found that transcription of CD59 was increased but vitronectin transcript expression was decreased in EOMD RPE cells (Fig. 6C). CD59 and vitronectin protein expression levels corresponded, respectively, with transcript expression (Figs. 6D, 6E). Clusterin was noted to be significantly increased in the ECM of EOMD RPE cells compared to controls and, to a lesser extent, increased intracellularly (Fig. 6E).

The expression of alternative pathway components, including C3, C5, CFB, CFI, and CFD, was also examined, and, although there were transcriptional level changes in CFD and CFB in EOMD RPE cells, these changes were not reflected in protein expression (Supplementary Fig. S5). An increase in intracellular CFB (L) protein expression in EOMD RPE cells was noted, although expression of CFD, CFI, and C5β was unchanged (Supplementary Fig. S5).

CRISPR/Cas9 Correction of the c.351-2A>G CFH Variant in EOMD RPE Cells Restores CFH/FHL-1 Expression and AP Complement Activity

To determine whether restoring CFH/FHL-1 expression to baseline levels can ameliorate the increased local complement activity seen in EOMD RPE cells, we generated CRISPR/Cas9-corrected EOMD (cEOMD) RPE cells and quantified the expression of key complement components in the amplification loop of the alternative pathway from the media of normal control, EOMD, and cEOMD RPE cells (Supplementary Fig. S6). Expression of CFH and FHL-1 by cEOMD RPE cells was significantly increased compared to uncorrected EOMD, to levels similar to control iPSC RPE

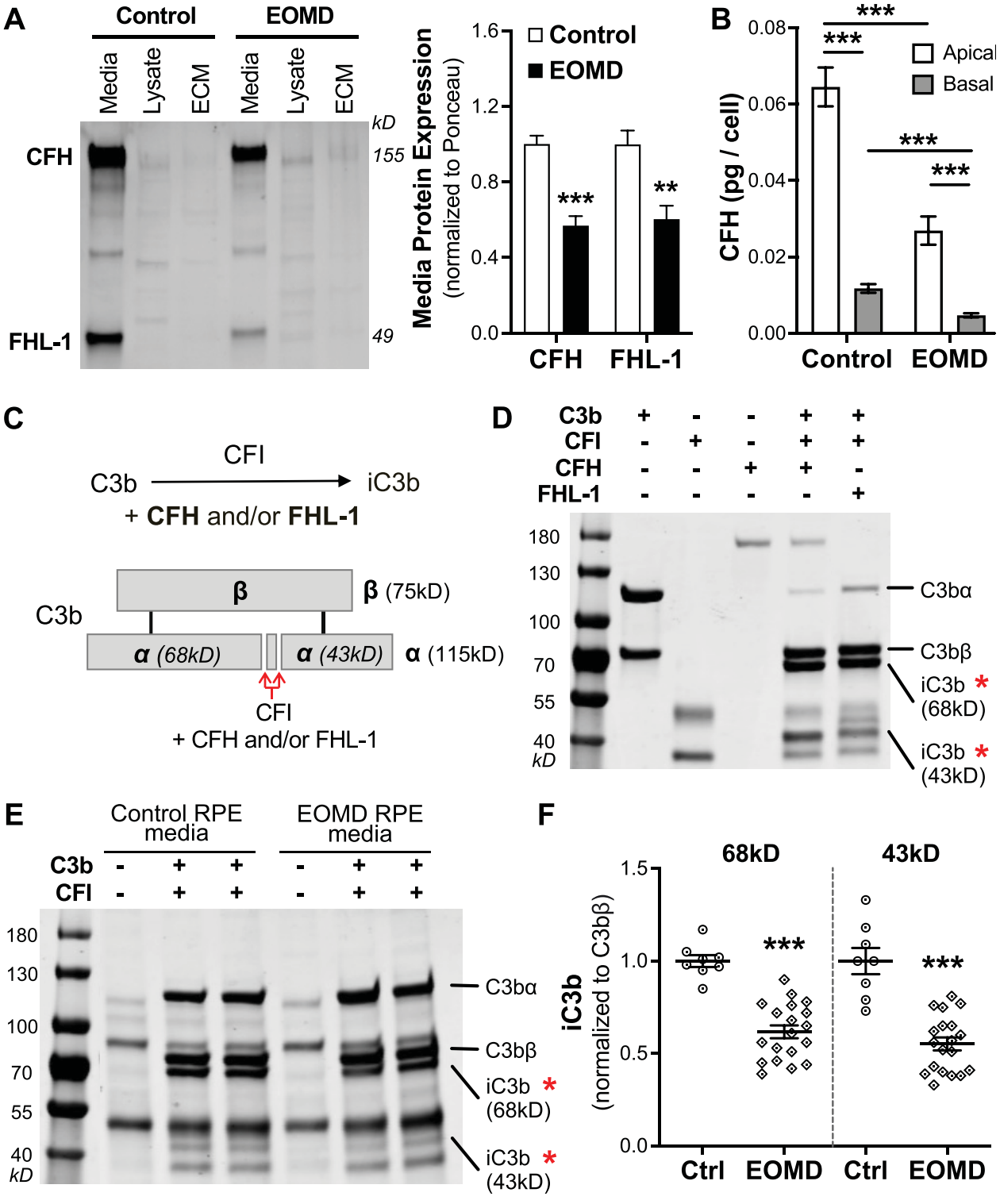

Figure 4. EOMD RPE cells had reduced CFH and FHL-1 secretion and co-factor activity. (**A**) CFH and FHL-1 proteins were largely secreted, with slight retention in the ECM. EOMD RPE cells had significantly reduced (~50%) CFH and FHL-1 compared to normal controls. (**B**) CFH ELISA performed on RPE cells cultured in filter inserts showed preferential basal secretion for CFH and confirmed >50% reduced secretion in both apical and basal directions in the EOMD RPE cells. (**C**) To assess CFH and FHL-1 co-factor activity, the in situ C3b breakdown assay was performed where CFH or FHL-1 was incubated with exogenous C3b and CFI for 15 minutes at 37°C. The reaction was terminated by the addition of SDS loading buffer and heated at 70°C for 10 minutes, then separated on an SDS-PAGE gel. (**D**) Successful C3bα cleavage results in the appearance of inactivated C3b (iC3b) at 68 kD and 43 kD (*). The C3bβ band is unchanged and used for normalization. (**E**) To perform this assay in RPE cultures, conditioned media from control and EOMD RPE cells cultures were collected, and 1 µg media protein was incubated with C3b and CFI. (**F**) iC3b was found to be significantly decreased in EOMD RPE cells compared to control RPE cells, indicating diminished co-factor activity in the EOMD RPE cells. *$P < 0.05$; ***$P < 0.001$ ($n = 3$).

Investigative Ophthalmology & Visual Science

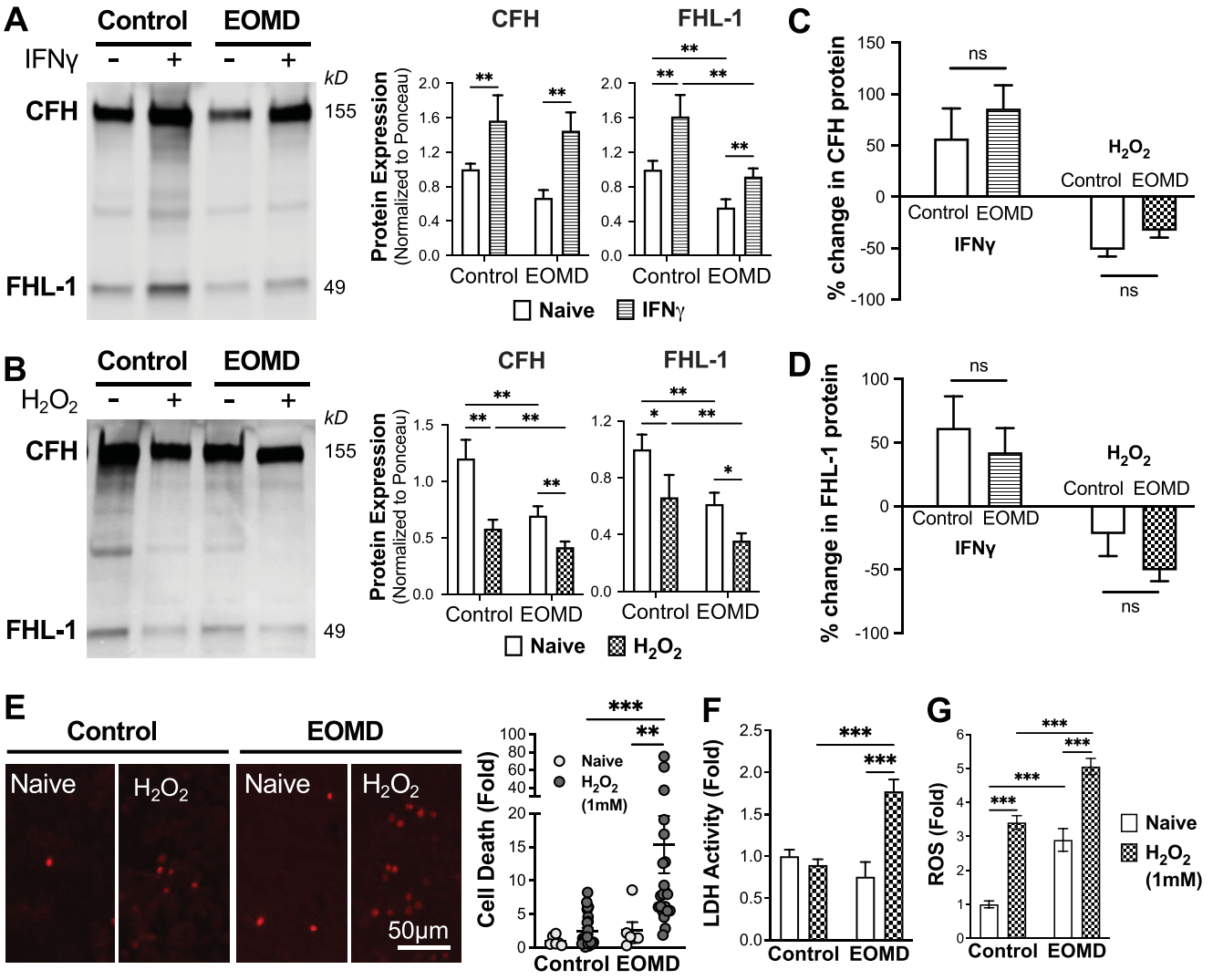

Figure 5. EOMD RPE cells had increased susceptibility to oxidative stress, but CFH and FHL-1 regulation with stressors remain unchanged. (**A**) Control and EOMD RPE cells treated with IFN-γ (25 ng/mL) resulted in upregulation of CFH and FHL-1 expression. (**B**) Conversely, treatment with H_2O_2 (1 mM) for 48 hours resulted in decreased CFH and FHL-1 expression in both RPE groups. (**C**, **D**) The percent changes in CFH and FHL-1 expression were similar between control and EOMD RPE cells, indicating the absence of compensatory upregulation in the EOMD RPE cells. (**E**) When evaluated for cell death as a result of oxidative stress, H_2O_2 (1 mM)–treated EOMD showed significantly increased ethidium bromide staining. (**F**) This was also reflected by heightened LDH activity in the culture media. (**G**) Likewise, the H_2DCFDA assay found elevated levels of ROS in EOMD RPE cells at baseline, with significant increases as compared to control RPE cells following H_2O_2 treatment. *$P < 0.05$; **$P < 0.01$; ***$P < 0.001$ ($n = 3$).

cells (Fig. 7A, B). Higher levels of C3a, C3b (C3bα and C3bβ), and C3b breakdown products in culture media indicate increased local complement activation. EOMD RPE cells had significantly higher levels of C3a and C3bα fragments (C3bα–f) compared to controls, but cEOMD had lower C3bα, C3bβ, and C3b–f compared to uncorrected EOMD RPE cells (Fig. 7C). These findings suggest that increased activity in the amplification loop in EOMD RPE cells can be ameliorated by correction of the c.351-2A>G CFH variant and restoration of CFH/FHL-1 expression.

Discussion

Local complement dysregulation is closely associated with AMD, and pathogenic variants in CFH leading to EOMD may offer valuable mechanistic insights into disease pathogenesis. In this report, we identified a novel variant of CFH in an EOMD patient cohort that results in decreased CFH and FHL-1 expression. We observed reduced CFH and FHL-1 co-factor activity, elevated MAC deposition, and increased alternative pathway activation products, collectively indicating heightened complement activity in EOMD RPE cells. A detailed analysis of additional complement components revealed increased RCA expression, including CD59, CD55, and clusterin (Fig. 8). In response to inflammatory and oxidative stressors, CFH and FHL-1 expression was appropriate, although not compensatory, and EOMD RPE cells were more susceptible to oxidative stress. CRISPR/Cas9 gene correction restored CFH and FHL-1 expression, resulting in a corresponding decrease in complement activity. These findings indicate that the novel CFH genetic variant directly contributes to increased local complement activity, and CFH

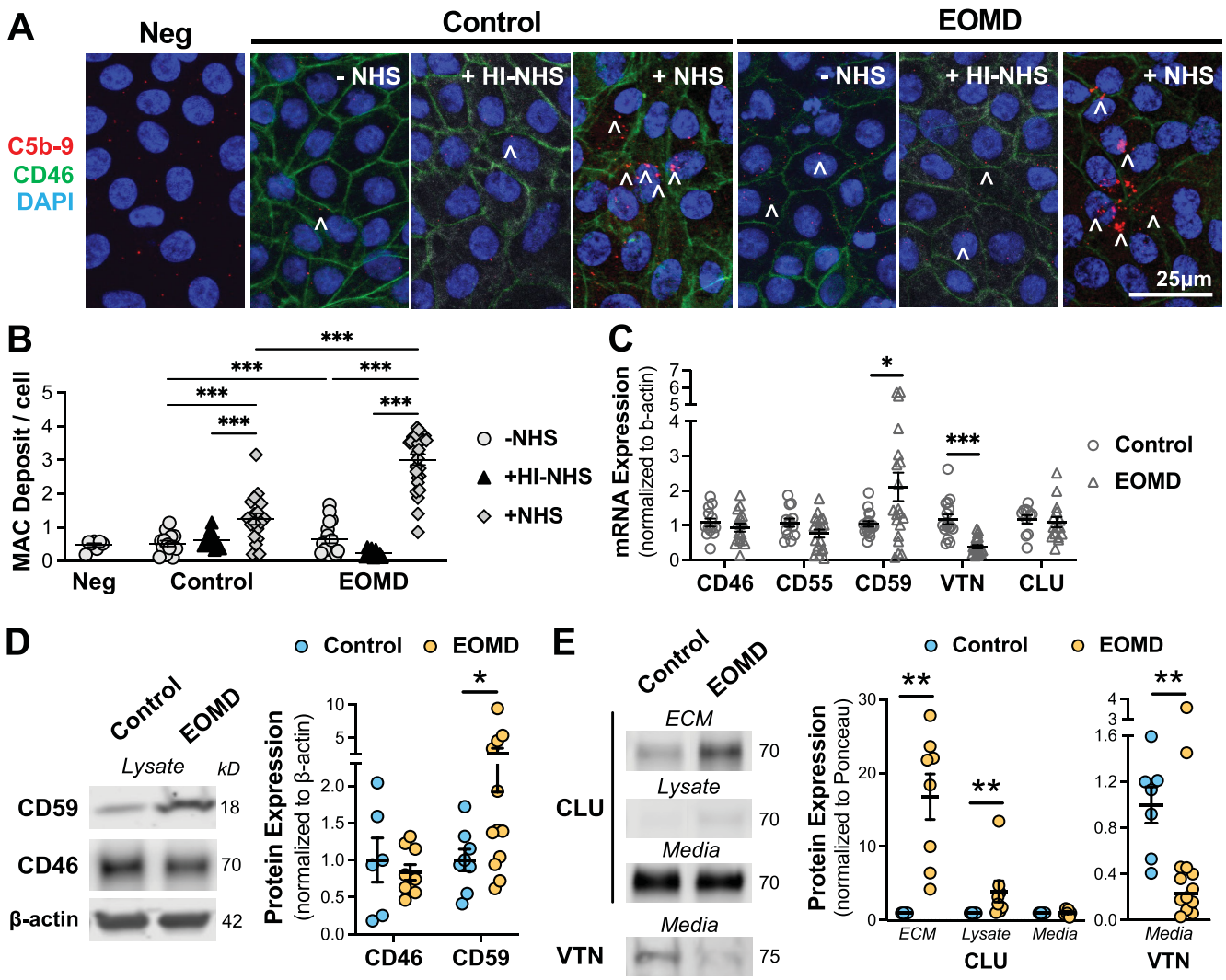

Figure 6. Local complement activity and RCA were increased in EOMD RPE cells. (**A**) RPE cells on chamber slides treated with 10% NHS or heat-inactivated (HI)-NHS for 24 hours were stained with C5b-9 (*red*) to identify MAC (^) and CD46 (*green*) to delineate the RCA on cell borders. To quantify true MAC deposits, the count of red puncta from images with secondary antibody only (Neg) was subtracted from all images. (**B**) The 10% NHS exposure resulted in MAC deposition in both control and EOMD RPE cells, although EOMD RPE cells had significantly increased deposits compared to control RPE cells, suggesting heightened local complement activity in the EOMD RPE cells. (**C**) Examination of five RCA member transcripts found increased CD59 and reduced vitronectin (VTN), with no changes in CD46, CD55, or clusterin (CLU). (**D**) Consistently, lysate CD59 was elevated in EOMD RPE cells, whereas CD46 showed no change in the lysate. (**E**) CLU expression was found to be mostly secreted, with significant increases in the ECM and lysate of EOMD RPE cells. VTN protein was also secreted with significant reductions in the EOMD RPE cells. $^{*}P < 0.05$; $^{**}P < 0.01$; $^{***}P < 0.001$ ($n = 4$).

gene supplementation in EOMD patients may be of potential therapeutic value.

Previous studies have shown that modulation of CFH levels can impact the health of RPE cells. Introducing recombinant human CFH into the culture media of ARPE-19 and iPSC-derived RPE cells protected against cell death and maintained tight junctions after exposure to oxidized lipids derived from photoreceptors, independent of MAC formation.[32] Conversely, CFH knockdown in hTERT–RPE1 cells induces inflammation[33] and reduces mitochondrial respiration and glycolysis.[27] These findings align with our observations of increased susceptibility to oxidative stress in EOMD RPE cells. Although CFH may confer protection to RPE cells, its expression can also be altered by extrinsic signals. IFN-γ[25] and IL-6,[34] mediators of the inflammatory pathway, and A2E,[35] a major fluorophore in lipofuscin, increase CFH secretion by RPE cells, whereas oxidative stressors such as H_2O_2,[26] cigarette smoke extract,[36] and blue light photooxidation[37] downregulate CFH expression. Although the pathogenesis of AMD likely results from a combination of stressors including deposit formation,[38] cellular impairment in mitochondrial function,[39] and autophagic flux,[40] the subnormal induction and suppression of CFH and FHL-1 expression in response to stressors may limit its ability to attenuate complement activity and protect against cell death, leading to an earlier onset of disease progression.

Compared to CFH, there is generally less information on RCA expression in AMD RPE pathology. CD59, a major cell surface inhibitor of MAC, is detectable in low levels in healthy human RPE cells,[41] elevated in iPSC–RPE cells generated from high-risk AMD donors,[40] elevated in macu-

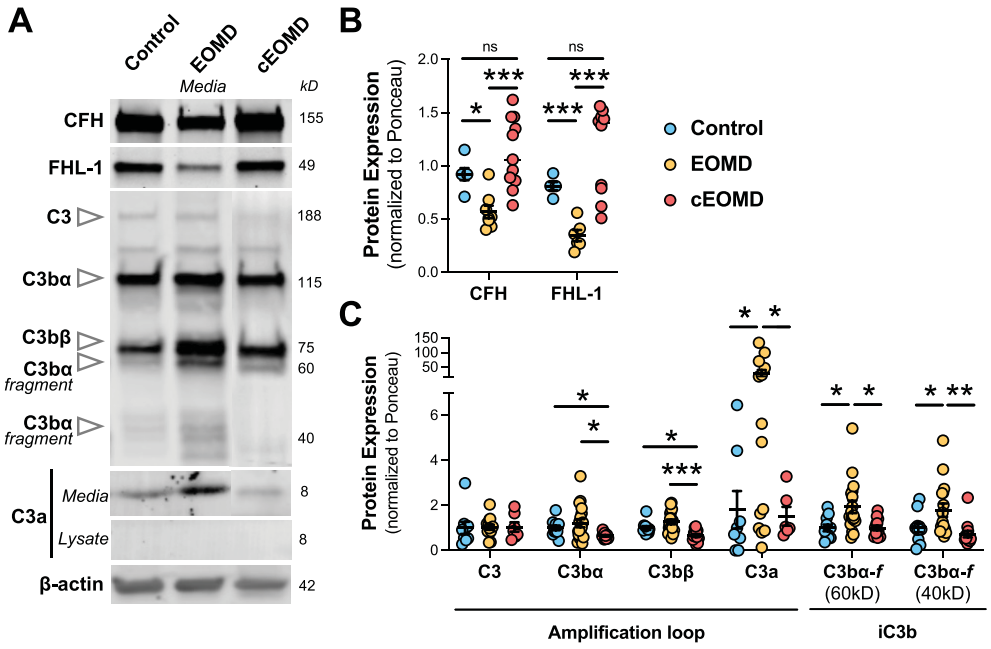

Figure 7. CRISPR/Cas9 correction restored CFH and FHL-1 expression and C3b turnover. (**A**, **B**) CFH and FHL-1 secretion from CRISPR-corrected (c)EOMD RPE cells were restored to levels similar to that of control RPE cells. (**C**) Western blot of C3 components in conditioned media found full-length C3 and C3b subunits C3bα and C3bβ to be unchanged in EOMD RPE cells. However, C3a and C3bα breakdown products, seen as 60-kD and 40-kD fragments on western blot were elevated, indicative of increased C3b turnover synonymous with complement activity in the EOMD RPE cells. These changes were ameliorated in cEOMD RPE cells to that of control RPE, suggesting that these effects are a result of CFH and FHL-1 insufficiency in the RPE cells ($n = 3$).

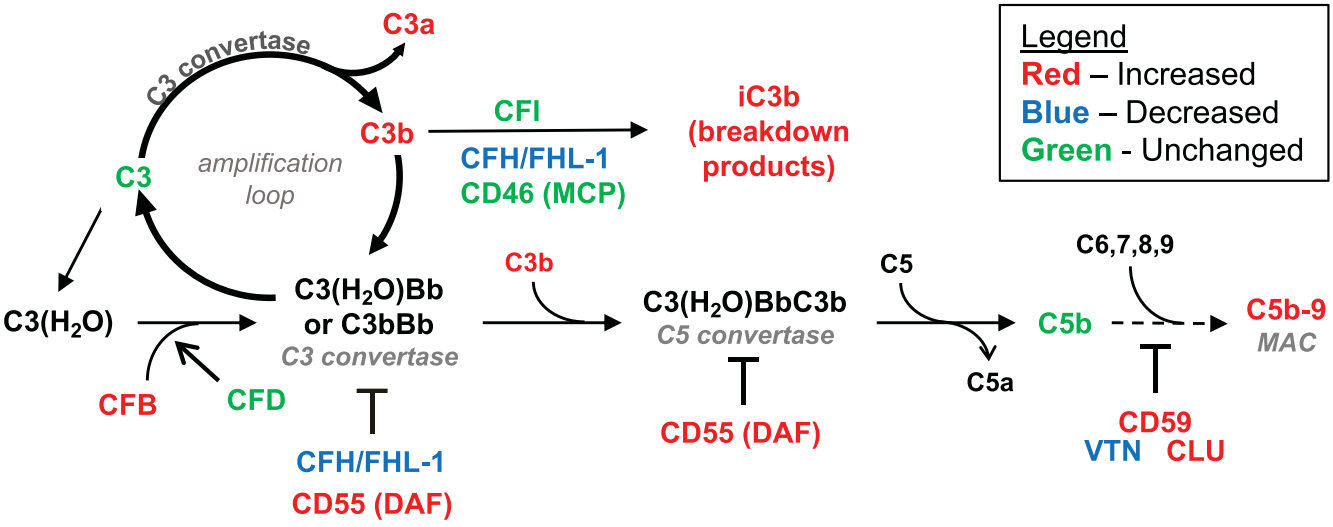

Figure 8. Increased local complement activity supported a role for CFH haploinsufficiency in EOMD disease pathogenesis. Loss of CFH and FHL-1 in EOMD RPE cells resulted in increased C3b turnover at the EOMD cell surface, amplifying complement activity and elevating compensatory expression of most RCA inhibitors, eventually leading to increased deposition of MAC on the EOMD RPE cells. *Red* indicates increased, *blue* indicates decreased, and *green* indicates unchanged.

lar tissue of early AMD globes, and entirely lost in atrophic areas overlying drusen.[41] In EOMD RPE cells, the increased CD59 transcript and protein expression was similar to what was found in AMD iPSC donor RPE cells and may reflect a compensatory response to increased local AP activity. Other RCA that diminish complement activation include vitronectin and clusterin, which bind to MAC and prevent cytolysis.[42] Although vitronectin was decreased in EOMD RPE media, future immunocytochemistry studies may be more revealing. Clusterin was significantly increased in the EOMD ECM. It is found in the drusen of AMD globes[11] and in basal laminar deposits[18] of iPSC–RPE models of AMD.[18,21,43] Initiating complement activation by exposure to NHS in control iPSC–RPE cells[38] and primary human RPE

cells[43] results in basal deposition, suggesting that increased complement activity may be a driver for clusterin deposition. Interestingly, despite an increase in RCA inhibitory components, MAC deposition in EOMD RPE cells was nevertheless higher than controls, perhaps highlighting the outsized influence of CFH and FHL-1 on local complement regulation.

The c.351-2A>G variant in this study, like many pathogenic CFH variants in EOMD, affects the highly conserved 3′ splice site, impacting the expression of both CFH and FHL-1. Although the size of full-length CFH (4 kb) precludes adeno-associated virus (AAV)-mediated gene supplementation, the smaller and mostly unglycosylated FHL-1 (1.8 kb) is considered the main complement regulator in Bruch's membrane and a potential therapeutic for reducing complement activity.[44] However, recent findings suggest that a truncated version of CFH containing the C-terminus, absent in FHL-1, may be sufficient for ocular complement regulation.[45] Although EOMD RPE cells showed ∼50% reductions in both CFH and FHL-1 expression, their individual contributions to increased AP activity were not investigated. EOMD RPE cells (and their isogenic controls) may serve as a disease-relevant model for exploration of CFH gene augmentation strategies. Other future opportunities include studying the effects of decreased CFH expression on its non-canonical roles in chemostasis,[25] cellular attachment,[46,47] modulation of lipoprotein binding,[48] upregulation of the pro-inflammatory pathway,[33] and cellular metabolism.[49] Finally, Müller glia, microglia, and retinal vascular cells are major contributors of complement activators in the neural retina, and apically secreted CFH may play a role in regulating subretinal complement activity.[50] Overcoming the technical challenges of including the neural retina and choroidal endothelium, which contributes significantly to local CFH and FHL-1,[50,51] would improve in vitro disease modeling.[52]

In conclusion, we showed that a novel CFH variant in patients with EOMD results in significant reduction in CFH and FHL-1 expression, increased local complement activation, appropriate but not compensatory expression in response to stressors, and increased susceptibility to oxidative stress in patient-derived iPSC RPE cells. Gene editing restored CFH/FHL-1 expression and mitigated alternative pathway complement activity in cEOMD RPE cells. These findings highlight the importance of CFH/FHL-1 expression in RPE health, providing insight into potential mechanisms of EOMD and AMD disease pathogenesis.

Acknowledgments

The authors thank the Tom and Sue Ellison Stem Cell Core for their assistance in CRISPR gene editing and generation of iPSC clones.

Supported by grants from the National Institutes of Health (EY034364 and EY034591 to JRC; EY001730 to NEI Vision Research Core) and the BrightFocus Foundation (M2020217 to JRC); by a BrightFocus Foundation Fellowship (M2023004F to RRL); by an Alcon Research Institute Senior Investigator Award (JRC); by a RPB Sybil B. Harrington Physician-Scientist Award for Macular Degeneration (JRC); and by an unrestricted grant from Research to Prevent Blindness.

Disclosure: **R.R. Lim**, None; **S. Shirali**, None; **J. Rowlan**, None; **A.L. Engel**, None; **M. Nazario, Jr.**, None; **K. Gonzalez**, None; **A. Tong**, None; **J. Neitz**, None; **M. Neitz**, None; **J.R. Chao**, None

References

1. Wong WL, Su X, Li X, et al. Global prevalence of age-related macular degeneration and disease burden projection for 2020 and 2040: a systematic review and meta-analysis. *Lancet Glob Health*. 2014;2:e106–e116.
2. Kleinman ME, Ambati J. Complement activation and inhibition in retinal diseases. *Dev Ophthalmol*. 2016;55:46–56.
3. Hageman GS, Anderson DH, Johnson LV, et al. A common haplotype in the complement regulatory gene factor H (HF1/CFH) predisposes individuals to age-related macular degeneration. *Proc Natl Acad Sci USA*. 2005;102:7227–7232.
4. Francis PJ, Hamon SC, Ott J, Weleber RG, Klein ML. Polymorphisms in C2, CFB and C3 are associated with progression to advanced age related macular degeneration associated with visual loss. *J Med Genet*. 2009;46:300–307.
5. Toomey CB, Johnson LV, Bowes Rickman C. Complement factor H in AMD: bridging genetic associations and pathobiology. *Prog Retin Eye Res*. 2018;62:38–57.
6. Voigt AP, Mulfaul K, Mullin NK, et al. Single-cell transcriptomics of the human retinal pigment epithelium and choroid in health and macular degeneration. *Proc Natl Acad Sci USA*. 2019;116:24100–24107.
7. Bhutto IA, Baba T, Merges C, Juriasinghani V, McLeod DS, Lutty GA. C-reactive protein and complement factor H in aged human eyes and eyes with age-related macular degeneration (AMD). *Br J Ophthalmol*. 2011;95:1323.
8. Demirs JT, Yang J, Crowley MA, et al. Differential and altered spatial distribution of complement expression in age-related macular degeneration. *Physiol Pharmacol*. 2021;62:1–12.
9. Fett AL, Hermann MM, Muether PS, Kirchhof B, Fauser S. Immunohistochemical l ocalization of complement regulatory proteins in the human retina. *Histol Histopathol*. 2012;27:357–364.
10. Crabb JW, Miyagi M, Gu X, et al. Drusen proteome analysis: an approach to the etiology of age-related macular degeneration. *Proc Natl Acad Sci USA*. 2002;99:14682–14687.
11. Wang L, Clark ME, Crossman DK, et al. Abundant lipid and protein components of drusen. *PLoS One*. 2010;5:1–12.
12. Mannes M, Dopler A, Huber-Lang M, Schmidt CQ. Tuning the functionality by splicing: factor H and its alternative splice variant FHL-1 share a gene but not all functions. *Front Immunol*. 2020;11:1–8.
13. Curcio CA, Johnson M. Structure, function, and pathology of Bruch's membrane. In: Ryan SJ, ed. *Retina*, 5th ed. Philadelphia: Saunders; 2012:465–481.
14. Makou E, Herbert AP, Barlow PN. Functional anatomy of complement factor H. *Biochemistry*. 2013;52:3949–3962.
15. Clark SJ, McHarg S, Tilakaratna V, Brace N, Bishop PN. Bruch's membrane compartmentalizes complement regulation in the eye with implications for therapeutic design in age-related macular degeneration. *Front Immunol*. 2017;8:1778.
16. Friese MA, Hellwage J, Jokiranta TS, et al. Different regulation of factor H and FHL-1/reconectin by inflammatory mediators and expression of the two proteins in rheumatoid arthritis (RA). *Clin Exp Immunol*. 2000;121:406–415.
17. Taylor RL, Poulter JA, Downes SM, et al. Loss-of-function mutations in the CFH gene affecting alternatively encoded factor H-like 1 protein cause dominant early-onset macular drusen. *Ophthalmology*. 2019;126:1410–1421.
18. Engel AL, Wang Y, Khuu TH, et al. Extracellular matrix dysfunction in Sorsby patient-derived retinal pigment epithelium. *Exp Eye Res*. 2021;215:108899.
19. Buchholz DE, Pennington BO, Croze RH, Hinman CR, Coffey PJ, Clegg DO. Rapid and efficient directed differentiation of human pluripotent stem cells into retinal pigmented epithelium. *Stem Cells Transl Med*. 2013;2:384–393.

Investigative Ophthalmology & Visual Science

20. Brydon EM, Bronstein R, Buskin A, Lako M, Pierce EA, Fernandez-Godino R. AAV-mediated gene augmentation therapy restores critical functions in mutant PRPF31$^{+/-}$ iPSC-derived RPE cells. *Mol Ther Methods Clin Dev*. 2019;15:392–402.
21. Galloway CA, Dalvi S, Hung SSC, et al. Drusen in patient-derived hiPSC-RPE models of macular dystrophies. *Proc Natl Acad Sci USA*. 2017;114:E8214–E8223.
22. Gong J, Cai H, Noggle S, et al. Stem cell-derived retinal pigment epithelium from patients with age-related macular degeneration exhibit reduced metabolism and matrix interactions. *Stem Cells Transl Med*. 2020;9:364–376.
23. Zipfel PF, Skerka C. FHL-1/reconectin: a human complement and immune regulator with cell-adhesive function. *Immunol Today*. 1999;20:135–140.
24. Datta S, Cano M, Ebrahimi K, Wang L, Handa JT. The impact of oxidative stress and inflammation on RPE degeneration in non-neovascular AMD. *Prog Retin Eye Res*. 2017;60:201–218.
25. Kim YH, He S, Kase S, Kitamura M, Ryan SJ, Hinton DR. Regulated secretion of complement factor H by RPE and its role in RPE migration. *Graefes Arch Clin Exp Ophthalmol*. 2009;247:651–659.
26. Wu Z, Lauer TW, Sick A, Hackett SF, Campochiaro PA. Oxidative stress modulates complement factor H expression in retinal pigmented epithelial cells by acetylation of FOXO3. *J Biol Chem*. 2007;282:22414–22425.
27. Armento A, Honisch S, Panagiotakopoulou V, et al. Loss of complement factor H impairs antioxidant capacity and energy metabolism of human RPE cells. *Sci Rep*. 2020;10:10320.
28. Liszewski MK, Atkinson JP. Membrane cofactor protein (MCP; CD46): deficiency states and pathogen connections. *Curr Opin Immunol*. 2021;72:126–134.
29. Dho SH, Lim JC, Kim LK. Beyond the role of CD55 as a complement component. *Immune Netw*. 2018;18:e11.
30. Armento A, Ueffing M, Clark SJ. The complement system in age-related macular degeneration. *Cell Mol Life Sci*. 2021;78:4487–4505.
31. Kimberley FC, Sivasankar B, Paul Morgan B. Alternative roles for CD59. *Mol Immunol*. 2007;44:73–81.
32. Borras C, Canonica J, Jorieux S, et al. CFH exerts anti-oxidant effects on retinal pigment epithelial cells independently from protecting against membrane attack complex. *Sci Rep*. 2019;9:13873.
33. Armento A, Schmidt TL, Sonntag I, et al. CFH loss in human RPE cells leads to inflammation and complement system dysregulation via the NF-κB pathway. *Int J Mol Sci*. 2021;22:8727.
34. Weinberger AWA, Eddahabi C, Carstesen D, Zipfel PF, Walter P, Skerka C. Human complement factor H and factor H-like protein 1 are expressed in human retinal pigment epithelial cells. *Ophthalmic Res*. 2014;51:59–66.
35. Parmar VM, Parmar T, Arai E, Perusek L, Maeda A. A2E-associated cell death and inflammation in retinal pigmented epithelial cells from human induced pluripotent stem cells. *Stem Cell Res*. 2018;27:95–104.
36. Wang L, Kondo N, Cano M, et al. Nrf2 signaling modulates cigarette smoke-induced complement activation in retinal pigmented epithelial cells. *Free Radic Biol Med*. 2014;70:155–166.
37. Lau LI, Chiou SH, Jui-Ling CL, Yen MY, Wei YH. The effect of photo-oxidative stress and inflammatory cytokine on complement factor H expression in retinal pigment epithelial cells. *Invest Ophthalmol Vis Sci*. 2011;52:6832–6841.
38. Sharma R, George A, Nimmagadda M, et al. Epithelial phenotype restoring drugs suppress macular degeneration phenotypes in an iPSC model. *Nat Commun*. 2021;12:7293.
39. Ebeling MC, Geng Z, Kapphahn RJ, et al. Impaired mitochondrial function in iPSC-retinal pigment epithelium with the complement factor H polymorphism for age-related macular degeneration. *Cells*. 2021;10:789–789.
40. Cerniauskas E, Kurzawa-Akanbi M, Xie L, et al. Complement modulation reverses pathology in Y402H-retinal pigment epithelium cell model of age-related macular degeneration by restoring lysosomal function. *Stem Cells Transl Med*. 2020;9:1585–1603.
41. Ebrahimi KB, Fijalkowski N, Cano M, Handa JT. Decreased membrane complement regulators in the retinal pigmented epithelium contributes to age-related macular degeneration. *J Pathol*. 2013;229:729–742.
42. Menny A, Lukassen MV, Couves EC, Franc V, Heck AJR, Bubeck D. Structural basis of soluble membrane attack complex packaging for clearance. *Nat Commun*. 2021;12:6086.
43. Johnson LV, Forest DL, Banna CD, et al. Cell culture model that mimics drusen formation and triggers complement activation associated with age-related macular degeneration. *Proc Natl Acad Sci USA*. 2011;108:18277–18282.
44. Clark SJ, Schmidt CQ, White AM, Hakobyan S, Morgan BP, Bishop PN. Identification of factor H–like protein 1 as the predominant complement regulator in Bruch's membrane: implications for age-related macular degeneration. *J Immunol*. 2014;193:4962–4970.
45. Grigsby D, Klingeborn M, Kelly U, et al. AAV gene augmentation of truncated complement factor H differentially rescues ocular complement dysregulation in a mouse model. *Invest Ophthalmol Vis Sci*. 2023;64:25.
46. Choudhury R, Bayatti N, Scharff R, et al. FHL-1 interacts with human RPE cells through the a5b1 integrin and confers protection against oxidative stress. *Sci Rep*. 2021;11:14175.
47. Hellwage J, Kühn S, Zipfel PF. The human complement regulatory factor-H-like protein 1, which represents a truncated form of factor H, displays cell-attachment activity. *Biochem J*. 1997;326:321–327.
48. Toomey CB, Kelly U, Saban DR, Rickman CB. Regulation of age-related macular degeneration-like pathology by complement factor H. *Proc Natl Acad Sci USA*. 2015;112:E3040–E3049.
49. Merle DA, Provenzano F, Jarboui MA, et al. mTOR inhibition via rapamycin treatment partially reverts the deficit in energy metabolism caused by FH loss in RPE cells. *Antioxidants*. 2021;10:1944.
50. Pauly D, Agarwal D, Dana N, et al. Cell-type-specific complement expression in the healthy and diseased retina. *Cell Rep*. 2019;29:2835–2848.e4.
51. Mulfaul K, Mullin NK, Giacalone JC, et al. Local factor H production by human choroidal endothelial cells mitigates complement deposition: implications for macular degeneration. *J Pathol*. 2022;257:29–38.
52. Song MJ, Quinn R, Nguyen E, et al. Bioprinted 3D outer retina barrier uncovers RPE-dependent choroidal phenotype in advanced macular degeneration. *Nat Methods*. 2023;20:149–161.

Investigative Ophthalmology & Visual Science